Synthesis of Chitosan Beads as Boron Sorbents

Elif Ant Bursalı, Yoldaş Seki, Serap Seyhan, Merve Delener, Mürüvvet Yurdakoç

Dokuz Eylül University, Faculty of Arts and Sciences, Department of Chemistry, 35160 Buca-Izmir, Turkey

Received 17 November 2007; accepted 26 August 2010
DOI 10.1002/app.33331
Published online 5 May 2011 in Wiley Online Library (wileyonlinelibrary.com).

ABSTRACT: Parameters, such as pH, temperature, initial boron concentration, adsorbent dosage, and ionic strength, affecting boron adsorption onto chitosan beads were examined in this study. The following values were obtained as the optimum conditions in our studied ranges: pH 8.0, temperature = 308 K, amount of chitosan beads = 0.15 g, initial boron concentration = 4 mg L^{-1}, and ionic strength = 0.1 *M* NaCl]. The adsorption kinetics were also examined in terms of three kinetic models: the pseudo-first-order, pseudo-second-order, and intraparticle diffusion models. The pseudo-second-order kinetic model showed very good agreement with the experimental data. Intraparticle plots seemed to have two steps and indicated multilinearity. Equilibrium data were evaluated with nonlinear and linear forms of the Langmuir and Freundlich equations. The experimental data conformed to the Freundlich equation on the basis of the formation of multilayer adsorption. To characterize the synthesized chitosan beads, we used Fourier transform infrared (FTIR) spectroscopy and scanning electron microscopy (SEM) analyses. As shown by FTIR analysis, the boron species may have interacted with the NH_2 groups on chitosan. Microparticles of about 5 μm appeared in the SEM micrographs of the chitosan beads. © 2011 Wiley Periodicals, Inc. J Appl Polym Sci 122: 657–665, 2011

Key words: FT-IR; gels; hydrogels

INTRODUCTION

High levels of boron are found in groundwater in areas associated with geothermal activity.[1] Boron contamination is also a source of human pollution. Boron compounds are used in a wide range of industrial applications, and high concentrations have been reported in industrial discharge.[1,2] Boron may pass into drinking water and irrigation water. Boron, of the seven essential micronutrient elements required for the normal growth of most plants, has a marked effect on plants in terms of both nutrition and toxicity. There is a relatively narrow range of soil boron concentrations between the level required for growth and the toxic level.[3–8] The boron concentration recommended for irrigation water was 0.75 mg L^{-1}.[9] The concentration range of boron in drinking water is judged to be between 0.1 and 0.3 mg L^{-1}, according to the guidelines for drinking water quality of the World Health Organization.[10] There is no easy method for removing boron from water.[11] The development of ecologically and economically appropriate technologies to remove toxic compounds of boron from different waters is a pressing goal over the entire world.[12]

Correspondence to: Y. Seki (yoldas.seki@deu.edu.tr).
Contract grant sponsor: Research Foundation of Dokuz Eylul University; contract grant number: 05-KB-FEN-052.

Orthoboric acid (H_3BO_3) is a very weak acid with a pK_a of 9.2 and, therefore, is not very susceptible to the transfer of protons in an aqueous solution. When $B(OH)_3$ ionizes in distilled water, $B(OH)_4^-$ and H_3O^+ are formed, and at higher pH values, the ratio of borate anion increases. The anion concentration in solution is pH-dependent. At pH values around 9.0, the $B(OH)_3$ and $B(OH)_4^-$ concentrations are practically the same, whereas at higher pH values (11.0), $B(OH)_4^-$ is the predominant species (pK_a = 9.2):[13,14]

$$B(OH)_3 + OH^- \rightarrow B(OH)_4^-$$

Chitosan, poly(*b*-1-4)-2-amino-2-deoxy-d-glucopyranose (Fig. 1), is produced by the partially alkaline *N*-deacetylation of chitin, which is found widely in the exoskeletons of shellfish and crustaceans and is the second most abundant natural biopolymer after cellulose.[15] Therefore, chitosan obtained from chitin is considered a relatively cheap material. Chitosan in the form of swollen beads has been found to exhibit a better adsorption capacity than flakes.[16] The amino (—NH_2) and hydroxyl (—OH) groups on the biopolymer chain of chitosan may be recognition and sorption sites for adsorbates. The electrolytic nature and chelating ability of biopolymers is mainly governed by the protonation degree of the —NH_3^+ group (pK_a = 6.3), which is dependent on pH.[17,18]

The aim of this study was to investigate the boron removal efficiency of chitosan beads as relatively cheap and ecological adsorbents from aqueous solutions. The

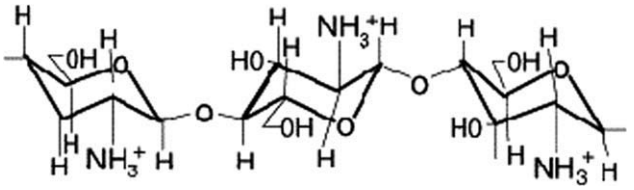

Figure 1 Molecular structure of chitosan.

effects of temperature, pH adsorbent dosage, and ionic strength on adsorption were also examined. The kinetics and adsorption isotherm parameters were also calculated from the adsorption data.

EXPERIMENTAL

Materials

Boric acid was supplied from Merck Co (Germany). A 100 mg L^{-1} boric acid stock solution was prepared by the dissolution of boric acid in distilled water. Working solutions were freshly prepared from the stock solution. Chitosan (low viscous), a flaked material, was obtained from Fluka (USA) (degree of deacetylation = 75–85%, average molecular weight = 500,000–700,000). HCl, NaCl, CH_3COOH, and NaOH were analytical grade and were purchased from Merck. The pH of the solutions was measured with a WTW pH meter (Germany) with an accuracy of ±0.1.

Preparation of the chitosan beads

The chitosan solution was prepared by the dissolution of 2.0 g of chitosan flakes into 50 mL of a 5% (v/v) acetic acid solution. It took about 24 h to dissolve chitosan completely. Then, the solution was dropped into 0.5*M* NaOH with pipette tips. The NaOH solution neutralized the acetic acid within the chitosan gel and, thereby, coagulated the chitosan gel to obtain special uniform chitosan gel beads. The wet chitosan gel beads were rinsed extensively with distilled water to remove any NaOH, filtered, and finally, freeze-dried to remove the water from the pore structure. The beads were then ground with a grinder and sieved to a constant size before use.

Adsorption experiments

To calculate the amount of adsorbed boron, batch adsorption experiments were conducted at different temperatures (298, 308, and 318 K). 0.05 g of chitosan beads was added to a capped volumetric flask containing 25 mL of boric acid solution at different concentrations (1–12 mg L^{-1} boron at a natural pH of 5.6). The flasks were shaken at 150 rpm for 30 min at different temperatures with a Memmert shaker (Germany). After the adsorption reached equilibrium, the samples were centrifuged, and the equilibrium boron concentration in the supernatant was measured by the newly developed azomethine-H-fluorimetric method in a Varian Cary Eclipse spectrofluorometer (Varian Inc., Palo Alto, USA).[19] The effect of pH on the adsorption of boron was also analyzed. The pH of the solution was adjusted with dilute HCl and NaOH solutions. For kinetic studies, 0.05 g of chitosan beads was used, and the amount of adsorbed boron was obtained at appropriate time intervals. The effect of the adsorbent dosage (0.05, 0.1, 0.15, 0.2, 0.25, and 0.3 g of chitosan beads) on the amount of adsorbed boron was determined with 10 mg L^{-1} boron solutions at 298 K (at natural pH). The effect of the ionic strength was also investigated with 0.1, 0.01, and 0.001*M* NaCl solutions [0.05 g of chitosan, temperature (T) = 298 K]. Finally, the adsorption experiments were carried out at the optimum values of pH, temperature, initial boron concentration, adsorbent dosage, and ionic strength.

Characterization of the chitosan beads

Fourier transform infrared (FTIR) analyses of the chitosan beads and boron-adsorbed chitosan beads were performed in a Spectrum BX-II PerkinElmer FTIR spectrophotometer (USA) with KBr pellets; the spectra were recorded in the range 4000–400 cm^{-1}. KBr (100 mg) was mixed with 1 mg of chitosan beads and boron-adsorbed chitosan beads.

To observe the microparticles (beads), scanning electron microscopy (SEM) analysis of the chitosan beads was conducted in a JEOL JSM 60 scanning electron microscope (Japan) and an X-ray energy-dispersive spectrometer. The surface morphologies of the chitosan beads were studied with a scanning electron microscope at an accelerating voltage of 10 kV.

RESULTS AND DISCUSSION

Effect of the contact time

The effect of the contact time on boron adsorption was measured at some time intervals and is shown in Figure 2. The boron adsorption attained equilibrium within 30 min at the studied temperatures. This was considered a relatively short time. It carried great weight for the removal rate of boron. For boron adsorption, it was reported that 120 min was enough time to reach the equilibrium state with layered double hydroxides and 24 h was enough for fly ash.[20,21] In our previous study, 100 min for the optimum contact time was observed with Siral samples.[22] Also, Öztürk and Köse[23] examined boron removal from an aqueous solution with a Dowex 2 × 8 anion exchange resin. They concluded that the equilibrium time was attained in 480 min at 298 K, 240 min at 308 K, and 15 min at 318

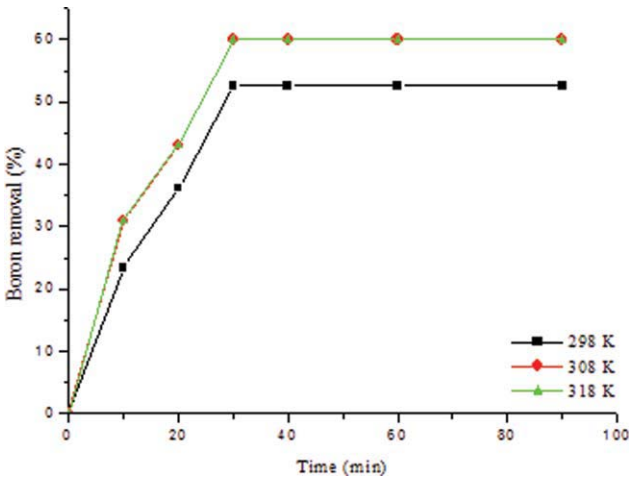

Figure 2 Effect of the contact time at different temperatures (mass of adsorbent = 0.05 g, pH = 5.6, initial boron concentration = 10 mg L^{-1}). [Color figure can be viewed in the online issue, which is available at wileyonlinelibrary.com.]

K.[23] Chitosan beads show relatively faster sorption kinetics at room temperature.

Of particular interest to us, as shown in Figure 2, the adsorption of boron at 308 and 318 K followed the same pattern. Therefore, the curve at 308 K could not be seen properly. We inferred that beyond 308 K, increasing temperature did not affect the amount of adsorption in the studied range of temperature. The percentage removal values of boron were determined to be 53, 60, and 60% at 298, 308, and 318 K, respectively. However, Öztürk and Köse[23] found that the percentage removal values of boron by the Dowex 2 × 8 anion exchange resin were 55, 40, and 33% at 298, 308, and 318 K, respectively.

Adsorption kinetics

To determine the sorption kinetics, the fit of the adsorption data to different kinds of kinetics models was examined. The kinetics of adsorption were interpreted with a pseudo-first-order equation and a pseudo-second-order model as follows:

$$\frac{1}{q_t} = \left(\frac{k_1}{q_1}\right)\left(\frac{1}{t}\right) + \frac{1}{q_1}$$

$$\frac{t}{q_t} = \frac{1}{k_2 q_2^2} + \frac{t}{q_2}$$

where q_t is the amount of adsorbed boron (mg g^{-1}) at time t (min); q_1 and q_2 are the maximum adsorption capacities (mg g^{-1}) for the pseudo-first-order and pseudo-second-order kinetic models, respectively;[24] and k_1 (min^{-1}) and k_2 (g mg^{-1} min^{-1}) are the rate constants for the pseudo-first-order and pseudo-second-order kinetic models, respectively.[25–27]

The fit of each model and the rate constants were obtained by the linear plot of $1/q_t$ versus $1/t$ and t/q_t versus t, respectively. From the slopes and intercept values of the plots, the k_1, k_2, q_1, and q_2 values were calculated.

The initial rate of adsorption ($h_{o,2}$) was also calculated as follows:

$$h_{o,2} = k_2 q_2^2$$

The kinetic parameters are presented in Table I. According to the correlation coefficients, we concluded that the pseudo-second-order kinetic model provided a better fit than the pseudo-first-order kinetic model. As shown in Table I, the rate constant values for the pseudo-second-order kinetic model at 308 and 318 K were the same. Beyond 308 K, increases in the temperature made no difference in terms of the rate constants and adsorption capacities in the studied range. As shown in Table I, the experimental adsorption capacity ($q_{e,\exp}$) values agreed well with the calculated ones, q_1 and q_2. However, the values of the sorption capacity (q_2) calculated from the pseudo-second-order kinetic model were closer to the values observed experimentally, $q_{e,\exp}$. Therefore, the pseudo-second-order kinetic model was more suitable than the pseudo-first-order kinetic model for describing the adsorption processes. The pseudo-kinetic models are better considered as empirical equations that do not reflect the actual chemical and physical phenomena taking place. With that in mind, the pseudo-kinetic models are still valuable as simple equations that predict the kinetics of adsorption systems and can be used in the design of adsorption units.[28]

When temperature was varied from 298 to 318 K, the value of $h_{o,2}$ increased from 0.2 to 0.3 mg g^{-1} min^{-1}. However, increases in the temperature beyond 318 K did not change $h_{o,2}$.

TABLE I
Kinetic Parameters for Boron Sorption onto the Chitosan Beads

Model	298 K	308 K	318 K
Pseudo-first-order model			
$q_{e,\exp}$	2.6	3.0	3.0
q_1 (mg g^{-1})	3.8	3.9	3.9
k_1 (min^{-1})	21.7	14.7	14.7
R^2	0.96	0.96	0.96
Pseudo-second-order model			
$h_{o,2}$(mg min^{-1} g^{-1})	0.2	0.3	0.3
q_2 (mg g^{-1})	3.1	3.4	3.4
$k_2 \times 10^2$ (g mg^{-1} min^{-1})	2.4	2.9	2.9
R^2	0.99	0.99	0.99
Intraparticle diffusion model			
k_p (mg g^{-1} $min^{-1/2}$)	0.22	0.22	0.22
R^2	0.64	0.64	0.64

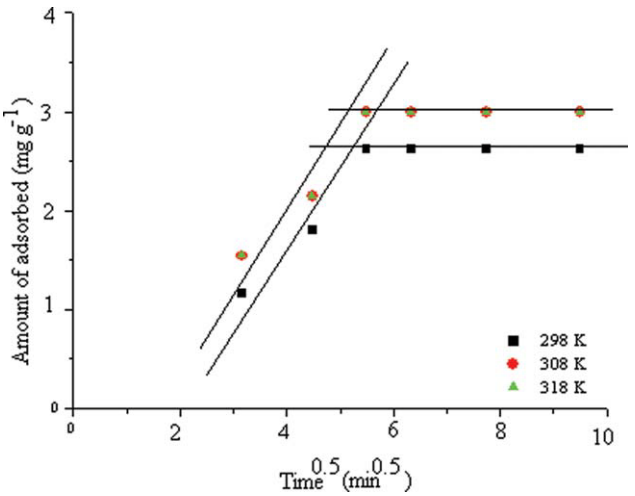

Figure 3 Intraparticle diffusion plots for the adsorption of boron onto chitosan beads. [Color figure can be viewed in the online issue, which is available at wileyonlinelibrary.com.]

The intraparticle diffusion model was applied to the experimental data of boron sorption onto the chitosan beads. The intraparticle diffusion model, which is considered a rate-limiting step, can be described by the following equation:

$$q_t = k_p t^{1/2} + c$$

where k_p is the intraparticle rate constant (mg g^{-1} $min^{-1/2}$) and c is the intercept. The calculated k_p values at different temperatures are given in Table I. The intraparticle plots are given in Figure 3. Clearly, the plots were not linear over the whole time range; this indicated that more than one process affected boron adsorption onto the chitosan beads. In the event that the initial part passed through origin, the intraparticle diffusion was the only rate-controlling step. As shown in the intraparticle plots, there were two steps that indicated multilinearity. The first one was steeper and showed the diffusion of borate species through the solution to the external surface of the chitosan beads or the boundary layer diffusion of solute molecules. Namely, during the first period, sorption was generated more easily, and the borate species may have moved at a faster speed. Also, in this stage, both the film and pore (intraparticle) diffusions may have been the rate-limiting step. The second portion of plot was almost parallel; this suggested equilibrium. In other words, the movement of boron species into the pores was restricted. Presumably, the borate species rapidly entered the macropores and wider mesopores and then may have penetrated more slowly into smaller mesopores. This signified that the intraparticle diffusion of the boron species into small mesopores was the rate-limiting step in the adsorption process.[26]

Adsorption isotherms

The adsorption isotherms for boron adsorption onto the chitosan beads are given in Figure 4, which is plotted the amount of adsorbed boron (C_s; mg g^{-1}) versus the equilibrium concentration (C_e; mg L^{-1}). At a higher initial concentration of boron solution (>2 mg L^{-1}), the greatest adsorbed boron was observed at 308 K. Moreover, in the initial concentration range between 2 and 12 mg L^{-1}, the lowest adsorbed boron was determined at 318 K. It is known that the relationship between adsorbed boron and boron concentration in solution can be revealed by various adsorption isotherm models. The most common adsorption models used to describe experimental data are the Freundlich and Langmuir models. The original forms of the Langmuir and Freundlich equations, respectively, are as follows:

$$C_s = \frac{C_m L C_e}{1 + L C_e}$$

$$C_s = K_f {C_e}^{nf}$$

where C_m is the monolayer capacity (mg g^{-1}), L is a constant (a function of the enthalpy of adsorption and temperature), K_f is the relative adsorption capacity (mg g^{-1}), and n_f is a measurement of linearity. In short, the linearized forms of these equations can be revealed, respectively, as follows:

$$\frac{C_e}{C_s} = \frac{1}{C_m L} + \frac{C_e}{C_m}$$

$$\ln C_s = \ln K_f + n_f \ln C_e$$

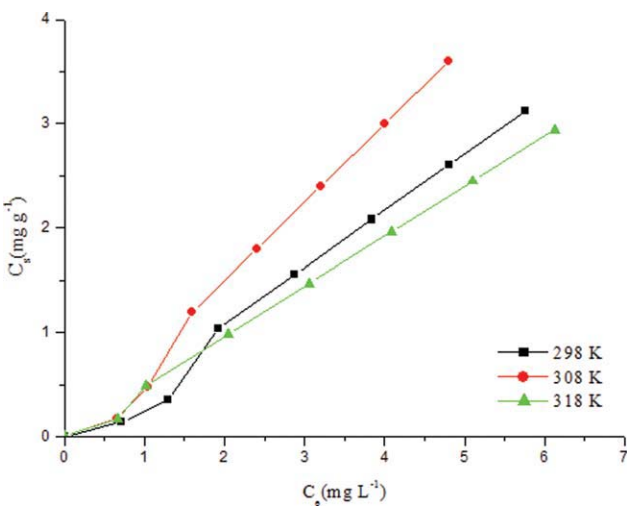

Figure 4 Adsorption isotherms for boron adsorption onto chitosan beads at different temperatures. [Color figure can be viewed in the online issue, which is available at wileyonlinelibrary.com.]

TABLE II
Adsorption Isotherm Parameters for Boron Adsorption onto the Chitosan Beads

	298 K	308 K	318 K
Linear form of the Langmuir equation			
C_m (mg g^{-1})	−2.0	−2.5	−5.7
L (L mg^{-1})	−0.12	−0.14	−0.06
R^2	0.55	0.56	0.29
Linear form of the Freundlich equation			
K_f (mg g^{-1})	0.3	0.4	0.4
n_f	1.49	1.47	1.13
R^2	0.97	0.97	0.97
Nonlinear form of the Langmuir equation			
C_m (mg g^{-1})	−18.4	−24.5	−89.8
L (L mg^{-1})	−0.03	−0.03	−0.01
R^2	0.98	0.98	0.99
Nonlinear form of the Freundlich equation			
K_f (mg g^{-1})	0.5	0.6	0.5
n_f	1.08	1.12	1.03
R^2	0.98	0.99	0.99

The plots of C_e/C_s versus C_e and ln C_s versus ln C_e give a straight line with slope values of $1/C_m$ and n_f; intercepts of $1/C_mL$ and ln K_f, respectively. Because of the inherent bias resulting from linearization, alternative isotherm parameters were found by nonlinear regression. This provides a mathematically rigorous method for determining isotherm parameters with the original form of the equation.[29] The parameters calculated with the linear and nonlinear forms of the Langmuir equation and linear and nonlinear forms of the Freundlich equation are summarized in Table II. As shown in Table II, the Freundlich equation provided better conformity than the Langmuir equation. Also, the nonlinear form of the Freundlich equation gave a better fit than the linear form of the Langmuir equation. The nonlinear form of the Freundlich equation provided a straight line with correlation coefficients of 0.98, 0.99, and 0.99 at 298, 308, and 318 K, respectively. K_f was calculated to be 0.48 mg g^{-1} for the nonlinear Freundlich equation at 298 K. In our previous studies, K_f values of 1.3, 0.3, 0.6, 0.1, 0.2, and 0.1 mg g^{-1} were obtained for bentonite, sepiolite, illite, Siral 5, Siral 40, and Siral 80, respectively.[22,30] Chitosan beads had a greater adsorption capacity than the Siral samples. The removal of boron from aqueous solutions with red mud was investigated by Cengeloglu et al.,[31] who reported that the Freundlich K_f was 5.996 mg g^{-1}. Cotton cellulose was used as the biosorbent for boron removal by Liu et al.,[32] and they found a K_f value of 0.16 mg g^{-1} at pH 7.[33] Kavak[34] used calcined alunite for the removal of boron from aqueous solution and obtained a K_f value of 0.033 mg g^{-1} at pH 10. The K_f values for the adsorption of boron by different adsorbents are compared in Table III.

In this study, as the temperature was increased to 308 K, K_f also went up. However, as the temperature was increased from 308 to 318 K, K_f decreased. The temperature of 308 K was noticeably more suitable than the other studied temperatures in terms of adsorption capacity. Because the Freundlich model was derived to model the multilayer adsorption, we inferred that the adsorption of boron onto chitosan may have been multilayer adsorption. Namely, the sorption process could be considered physical sorption in this study. The n_f value, which is also known as the adsorption intensity, was determined to be greater than 1; this indicated an S-type isotherm and also mostly corresponded to physical adsorption.[27]

Effect of the pH

The effect of the initial pH on the removal of boron was determined, as given in Figure 5. It is known that the pH of the solution affects the distribution of boron species, such as $B(OH)_3$ and $B(OH)_4^-$. The boron adsorption depends on which boron species are dominant in the solution. The pK_a value of boric acid is 9.2, where half of the total boron is in the form of boric acid and half is in the form of borate anions. When the pH is below 9, $B(OH)_3$ is dominant in aqueous species.[29] The pH of the solution also affects the charge distribution of chitosan, which is a weak base with a pK_a value of the d-glucosamine residue of about 6.2–7.0. At low pH values, the NH_2 groups of chitosan are protonated, and NH_3^+ groups on

TABLE III
K_f Values for the Adsorption of Boron by Different Adsorbents

Adsorbent (g)	K_f (mg g^{-1})	pH	Temperature (°C)	Reference
Cotton cellulose	0.16 ($R^2 = 0.75$)	7	Room temperature	32
Cerium oxide	1.426 ($R^2 = 0.90$)	9	25	35
Calcined alunite	0.033 ($R^2 = 0.99$)	10	25	34
Çamlıca bentonite 1	0.05 ($R^2 = 0.997$)	10	45	19
Çamlıca bentonite 2	0.002 ($R^2 = 0.997$)	10	45	19
Neutralized red mud	5.996 ($R^2 = 0.99$)	7	25	31
Nonactivated waste sepiolite	8.34 ($R^2 = 0.865$)	10	20	36
HCl-activated waste sepiolite	14.13 ($R^2 = 0.91$)	10	20	36
Chitosan beads	0.3 ($R^2 = 0.97$)	8	25	This study

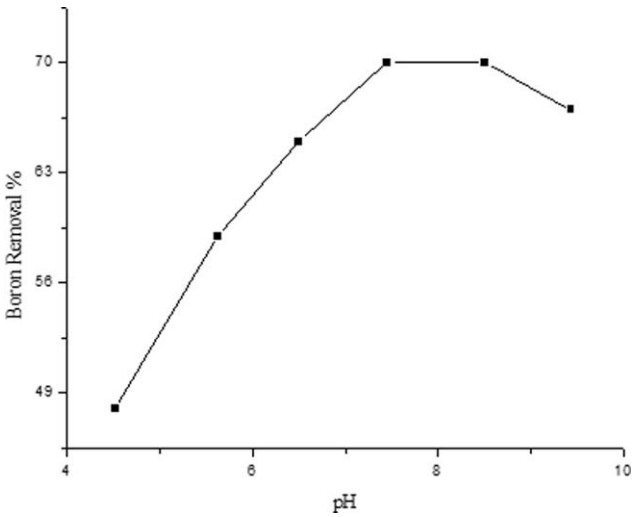

Figure 5 Effect of pH on the removal of boron from an aqueous solution (initial boron concentration = 10 mg L^{-1} boron, mass of adsorbent = 0.05 g, T = 298 K, volume = 25 mL).

chitosan are the dominant group compared to NH_2 groups. At high pH values, when the amount of protonated amine groups is decreased, the amount of neutral —NH_2 groups increases. As shown in Figure 5, boron removal increased when the pH of the solution was increased from 4.5 to 7.5, although in the range of pH of 7.5–8.5, boron removal remained constant at about 70%; this may be accepted as the maximum amount of adsorbed boron. The amount of boron removal at pH 4.5 was about 48%. At this pH value, there might have been slight interaction between the NH_3^+ groups on chitosan and $B(OH)_3$ species. Beyond a pH value of 8.5, the amount of boron removal decreased. In that pH range, the NH_2 groups on chitosan and the species of $B(OH)_4^-$ were considered the dominant groups. However, the OH^- concentration in the solution also increased. There may have been a competition between the negatively charged boron species and OH^-. Therefore, boron removal decreased after pH 8.5. In addition, the OH groups on chitosan may have behaved as sorption sites for boron species. Hydrogen bonds may have been formed between the OH groups on chitosan and boron species. Nevertheless, as pointed out previously, the NH_2 groups on chitosan may have been more efficient than the OH groups on chitosan for the removal of boron from aqueous solution.

Effect of the adsorbent dosage

The effect of the adsorbent dosage on boron removal is presented in Figure 6. The adsorbent dosages used in this study were between 0.05 and 0.30 g of chitosan beads. The adsorbent dosage increased the amount of boron removal in the adsorbent range 0.05–0.15. This may have been due to an increase in sorption sites for boron species. Beyond an adsorbent dose of 0.15 g, boron removal remained constant. This may have been due to the fact that equilibrium was reached in the solid–solution interface. Also, there was an equilibrium of boron species $B(OH)_3$ and $B(OH)_4^-$, and in a limit value of concentration, there will not be the conversion of $B(OH)_3$ to $B(OH)_4^-$.[20]

Ionic strength effect

The effect of the ionic strength is given in Figure 7. Different NaCl concentrations (0.1, 0.01, and 0.001M NaCl) were used to examine salt effects in this study. As shown in Figure 7, as the ionic strength increased, boron removal also increased. Along with increasing ionic strength, a very concentrated environment existed outside of the chitosan microparticles. A larger concentration of mobile ions outside the chitosan microparticles decreased the interactions between the chitosan beads and the solvent (water). In addition to this, as revealed by Sun et al.[37] for fulvic acid by chitosan beads, salt may screen the electrostatic interactions and may, especially, screen the mutual repulsion between the adsorbed boron species; hence, boron adsorption is enhanced with increasing salt concentration.

On the other hand, from the view of optimum conditions, the amount of adsorbed boron can be also expressed as shown in Figure 8. As shown in Figure 8, at the optimum conditions (T = 308 K, pH 8.0, boron concentration = 4 mg L^{-1}) without any salt, the boron removal was about 66%. However, in the presence of 0.1M NaCl under the same conditions, boron removal increased to 74%. In other words, the maximum amount of adsorbed boron in this study was 74%.

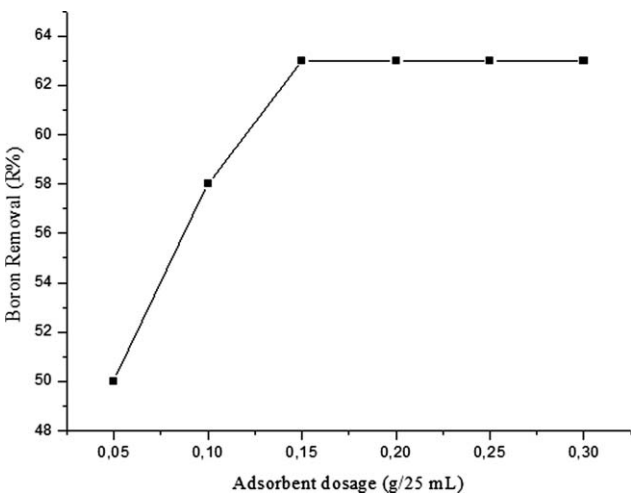

Figure 6 Effect of the adsorbent dosage on boron removal (T = 298 K, initial boron concentration = 10 mg L^{-1}).

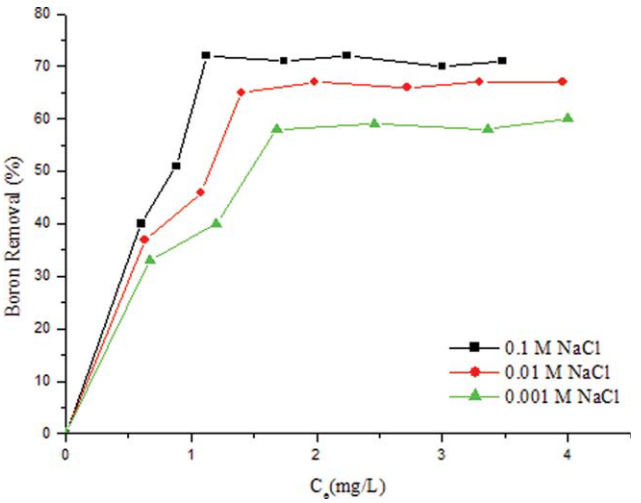

Figure 7 Effect of the ionic strength on boron removal (T = 298 K). [Color figure can be viewed in the online issue, which is available at wileyonlinelibrary.com.]

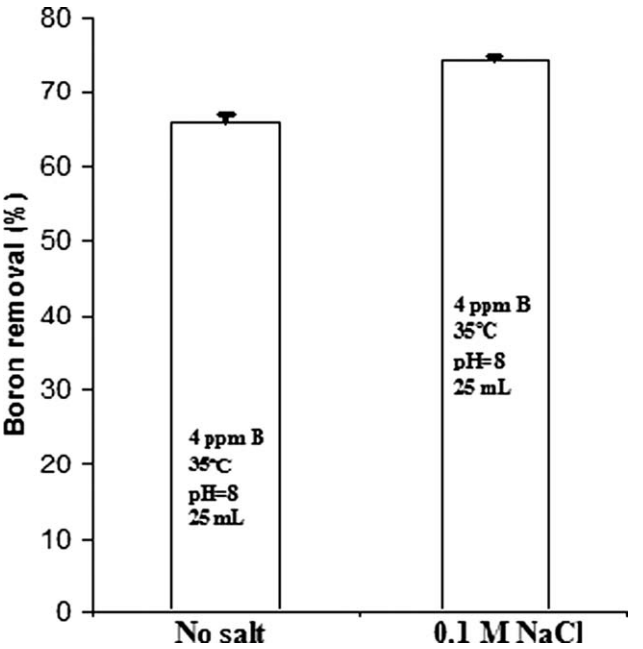

Figure 8 Boron removal at optimum conditions.

FTIR analysis

FTIR analyses of the chitosan beads and boron-adsorbed chitosan beads are given in Figure 9. We expected that we would find evidence for the adsorption of boron onto chitosan. In particular, recognition sites of chitosan for boron species could be determined. The strong band centered at 3428 cm^{-1} in the spectrum of the chitosan beads was assigned to the O—H stretching mode of chitosan. After boron adsorption, a broad band was observed. In addition to this, the O—H stretching vibration did not change significantly. This may have indicated that a weak interaction occurred between the boron species and OH groups of chitosan. Two shoulders at 3290 and 3177 cm^{-1} were attributed to the N—H stretching mode of chitosan. These shoulders could not be seen exactly in the spectrum of the chitosan beads with boron. Boron species may have interacted with the NH_2 groups of chitosan. The band located at 2923 cm^{-1} was identified as the C—H stretching vibration of the polymer backbone. This band slightly decreased to 2920 cm^{-1} after boron was adsorbed. The band at 1413 cm^{-1} in the spectrum of the chitosan beads was due to C—H bending. However, there were three different bands at 1419, 1381, and 1316 cm^{-1} in the spectrum of the chitosan beads with boron. According to Ay et al.,[38] broad B—O stretches of the trigonal borate appeared in the region 1300–1480 cm^{-1}. Therefore, the reason for the splitting of the band in the range 1300–1450 cm^{-1} may have been the B—O stretching of borate. However, the band at 1381 cm^{-1} may have been due to the B—N stretching vibration. This was considered to be evidence for the interaction between the chitosan and boron species. The band located at 1640 cm^{-1} in the spectrum of the chitosan beads was attributed to the amide I band, C=O stretching of the acetyl groups. N—H bending vibrations appeared at 1562 cm^{-1}. After boron adsorption, these bands increased to 1653 and 1599 cm^{-1}. The intensity of the N—H bending mode decreased as result of boron adsorption onto the chitosan beads. This also confirmed the interaction amino groups of the chitosan and boron species. Two bands, the first at 1154 cm^{-1} and the second at 1074 cm^{-1}, showed the C—O stretching mode of chitosan. After boron adsorption, the first one was almost the same; however, the second one demonstrated a small increase. In the spectrum of

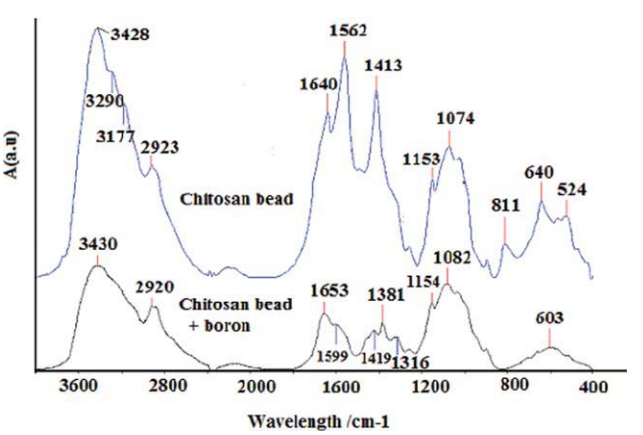

Figure 9 FTIR spectra of the chitosan beads and boron-adsorbed chitosan beads. [Color figure can be viewed in the online issue, which is available at wileyonlinelibrary.com.]

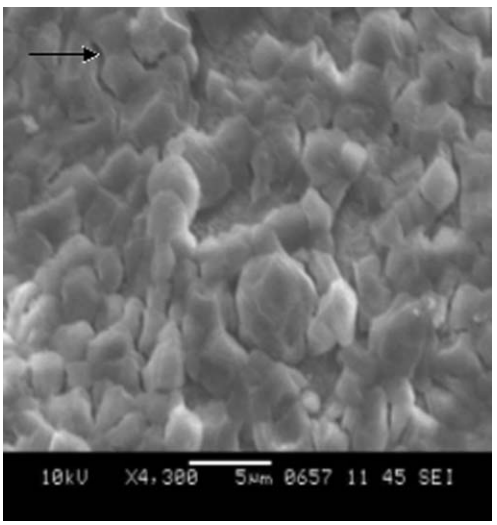

Figure 10 SEM micrographs of the chitosan beads.

chitosan, the presence of two bands, one at 1153 cm^{-1} and another at 1074 cm^{-1}, probably indicated the stretching vibrations of C—O groups. The first band did not demonstrate any changes. In the second band, a small change was observed. In summary, for the FTIR analysis, the NH_2 groups on chitosan may have acted as recognition sites for boron species, such as borate anion $B(OH)_4^-$ or boric acid.

SEM analysis of the chitosan beads

The concentration of NaOH was higher than that of acetic acid within the chitosan solution. Therefore, it is probable that NaOH reacted with protonated amino groups in the chitosan molecules and acetic acid molecules. As indicated by Zhao et al.,[15] liquid–liquid phase separation occurred; the chitosan gel was coagulated to generate porous spherical uniform chitosan gel beads with a skin layer. As presented in Figure 10, microparticles of about 5 μm (slightly greater and smaller) were observed inside the gel beads. Also, gaps (shown with an arrow in Fig. 10) smaller than 1 μm were seen among the microparticles, which adhered to each other.

CONCLUSIONS

The adsorption of boron onto chitosan beads was investigated at various temperatures, ionic strengths, and pH values. As the pH of the solution was increased up to 7.5, boron removal also increased. Beyond a pH of 7.5, boron removal remained constant at about 70%. A value of 0.15 g of adsorbent was obtained as the optimum adsorbent dosage. With increasing ionic strength, boron removal increased. Boron adsorption reached equilibrium within 30 min at the studied temperatures. Kinetic experiments showed that the adsorption of boron onto chitosan followed the pseudo-second-order kinetic model, and intraparticle diffusion was not the only rate-controlling step. From batch experiments, we concluded that the Freundlich equation agreed very well with the experimental data. Probably, the adsorption of boron species onto the chitosan beads occurred with physical forces. SEM analysis showed that microparticles of about 5 μm were observed inside the gel beads. As a result of FTIR analysis, we inferred that the NH_2 groups on chitosan may have acted as reaction sites for boron species. In conclusion, chitosan, as a relatively cheap, abundant, and nontoxic material, could be used for the removal of boron species from aqueous solution.

References

1. Okay, O.; Guclu, H.; Soner, E.; Balkas, T. Water Res 1985, 19, 852.
2. Morales, G. V.; Mercado Fuentes, M. E. L.; Quiroga, O. D. Hydrometallurgy 2000, 58, 127.
3. Duranceau, P. E.; Ditri, F. M. Tech Rep Water Res 1976, 44, 1.
4. Tazaki, T. Environmental Botany; Asakura: Tokyo, 1980.
5. Bingham, R. F. T. Adv Soil Sci 1985, 1, 229.
6. Wong, J. W. C.; Jiang, R. F.; Su, D. C. Soil Sci 1996, 161, 182.
7. Qian, J. H.; Zayed, A.; Zhu, Y. L.; Yu, M.; Terry, N. J. Environ Qual 1999, 28, 1448.
8. Fujita, Y.; Hata, T.; Nakamaru, M.; Iyo, T.; Yoshino, T.; Shimamura, T. Bioresour Technol 2005, 96, 1350.
9. Rowe, D. R.; Abdel-Magid, I. M. Handbook of Wastewater Reclamation and Reuse; Springer: Boca Raton, FL, 1995; p 550.
10. World Health Organization. Guidelines for Drinking-Water Quality, 3rd ed.; World Health Organization: Geneva, Switzerland, 2004; Vol. 1, Chapter 8.
11. Geffen, N.; Semiat, R.; Eisen, M. S.; Katz, Y. I.; Dosoretz, C. G. J Membr Sci 2006, 286, 45.
12. Melnyk, L.; Goncharuk, V.; Butnyk, I.; Tsapiuk, E. Desalination 2007, 205, 206.
13. Lou, J.; Foutch, G. L.; Jung, W. N. Sep Sci Technol 1999, 34, 2923.
14. Peak, D.; Luther, G. W.; Sparks, D. L. Geochim Cosmochim Acta 2003, 67, 2551.
15. Zhao, F.; Yu, B.; Zhengrong, Y.; Wang, T.; Wen, X.; Liu, Z.; Zhao, C. J Hazard Mater 2007, 147, 67.
16. No, H. K.; Meyers, S. P. Environ Contam Toxicol 2000, 163, 1.
17. Dambies, L.; Guimon, C.; Yiacoumi, S.; Guibal, E. Colloids Surf A 2001, 177, 203.
18. An, J. H.; Dultz, S. Appl Clay Sci 2007, 36, 256.
19. Seyhan, S.; Seki, Y.; Yurdakoc, M.; Merdivan, M. J Hazard Mater 2007, 146, 180.
20. Ferreira, O. P.; Moraes, S. G.; Duran, M.; Cornejo, L.; Alves, O. L. Chemosphere 2006, 62, 80.
21. Ozturk, N.; Kavak, D. J Hazard Mater B 2005, 127, 81.
22. Yurdakoc, M.; Seki, Y.; Karahan, S.; Yurdakoc, K. J Colloid Interface Sci 2005, 286, 440.
23. Öztürk, N.; Köse, T. E. Desalination 2008, 227, 233.
24. Seki, Y.; Yurdakoç, K. Adsorption 2006, 12, 89.

25. Malik, P. K. Dyes Pigments 2003, 56, 239.
26. Grabowska, E. L.; Gryglewicz, G. Dyes Pigments 2007, 74, 34.
27. Ho, Y. S.; McKay, G. Chem Eng J 1998, 70, 115.
28. Hameed, B. H.; El-Khaiary, M. I. J Hazard Mater 2008, 154, 639.
29. Seki, Y.; Seyhan, S.; Yurdakoc, M. J Hazard Mater B 2006, 138, 60.
30. Karahan, S.; Yurdakoc, M.; Seki, Y.; Yurdakoc, K. J Colloid Interface Sci 2006, 293, 36.
31. Cengeloglu, Y.; Tor, A.; Arslan, G.; Ersoz, M.; Gezgin, S. J Hazard Mater 2007, 142, 412.
32. Liu, R.; Ma, W.; Jia, C.; Wang, L.; Li, H. Desalination 2007, 207, 257.
33. Kose, T. E.; Ozturk, N. J Hazard Mater 2008, 152, 744.
34. Kavak, D. J Hazard Mater 2008, 163, 308.
35. Öztürk, N.; Kavak, D. Desalination 2008, 223, 106.
36. Öztürk, N.; Kavak, D. Adsorption 2004, 10, 245.
37. Sun, X. F.; Wang, S. G.; Liu, X. W.; Gong, W. X.; Bao, N.; Ma, Y. Colloids Surf A 2008, 324, 28.
38. Ay, A. N.; Karan, B. Z.; Temel, A. Micropor Mesopor Mater 2007, 98, 1.